RJC

RASĀYAN ***J. Chem.***
Vol. 18 | No. 2 |1138-1153| April - June | 2025
ISSN: 0974-1496 | e-ISSN: 0976-0083 | CODEN: RJCABP
http://www.rasayanjournal.com
http://www.rasayanjournal.co.in

SYNTHESIS, SPECTROSCOPIC CHARACTERISATION OF NOVEL METAL COMPLEXES OF AN INNOVATIVE CLASS OF MANNICH BASE AS LARVICIDES AGAINST *Culex quinquefasciatus* AND DOCKING STUDIES

Devaraj Kavitha[1,2], Velayutham Gurunathan[3], Karumalaiyan Palanisamy[4], and Sangilimuthu Aruna Devi[1,✉]

[1]PG and Research Department of Chemistry, Urumu Dhanalakshmi College (Affiliated to Bharathidasan University), Tiruchirappalli, Tamil Nadu, India - 620019.
[2]PG and Research Department of Chemistry, Government Arts College (Affiliated to Bharathidasan University), Ariyalur, Tamil Nadu, India – 621713.
[3]Research Department of Chemistry, Bishop Heber College (Affiliated to Bharathidasan University), Tiruchirappalli District, Tamil Nadu, India - 620017.
[4]Research Department of Chemistry, School of Engineering and Technology, Dhanalakshmi Srinivasan University, Perambalur Campus, Tamil Nadu, India - 621212.
✉Corresponding author: aruna07ravi@gmail.com

ABSTRACT

Lymphatic filariasis and malaria are among the utmost prevalent recognised parasitic illnesses spread by mosquitoes globally. Mosquito-borne diseases are estimated to cause around 1 million fatalities annually. Such illnesses are managed with the application of pesticides; yet, these may adversely affect non-target organisms. Consequently, we aimed to identify an appropriate larvicidal molecule to substitute pesticides by assessing the larvicidal efficacy of Mannich base ligand (**L1**) and its corresponding complexes (**1-5**) towards *Culex quinquefasciatus*. Five novel complexes were synthesised by using the bidentate ligand 5-(((2-aminoethyl)amino)(2-hydroxyphenyl)methyl)-2-thioxodihydropyrimidine-4,6(1H,5H)-dione (L1), which was produced via the condensation reaction of salicylaldehyde, ethylenediamine, and thiobarbituric acid (Mannich reaction) and various transition metal chlorides. The ligand and its complexes were characterised through molar conductivity, Nuclear Magnetic Resonance spectroscopy (^{1}H and ^{13}C NMR), magnetic susceptibility, Electron Paramagnetic Resonance spectroscopy (EPR), Ultraviolet-Visible spectroscopy (UV-Vis), and Fourier Transform-Infrared spectroscopy (FT-IR) assessments. The anticipated geometries of the complexes were proposed as octahedral, and they exhibit non-electrolytic characteristics. The larvicidal effect on the 4th instar *Culex quinquefasciatus* larvae was investigated at various concentrations of the ligand (**L1**) and its related complexes (**1-5**). The findings indicated that the Mn(II) complex exhibited the most significant larvicidal efficacy compared to all other complexes, while also demonstrating reduced toxicity to non-target aquatic organisms. Computational docking assessments were performed to assess the binding score of designed drugs to target proteins and to elucidate the mechanism of action at the binding pocket.

Keywords: Antifeedant, *Culex quinquefasciatus*, Larvicidal Activity, Magnetic Moment, Mannich Base, Metal Complexes, Molecular Docking.

RASĀYAN *J. Chem.*, Vol. 18, No. 2, 2025

INTRODUCTION

The Mannich reaction, recognized in 1917, is a notable multi-component reaction that involves the concurrent inclusion of an aldehyde, an amine, and a ketone in a single condensing process to yield amino carbonyl substances, which are referred to as Mannich bases.[1-6] The process is crucial since it enables the formation of novel C-C bonds, allowing for the production of various amino carbonyl compounds. Thus, the Mannich reaction substantially influences the production of important biomolecules, including amino acids, lactams, amino alcohols, peptides, and other physiologically relevant chemicals. Its variety and effectiveness in establishing essential biochemical connections render it a crucial and beneficial technique in contemporary organic synthesis; the resulting substances may serve as adaptable intermediates that

http://doi.org/10.31788/RJC.2025.1829139

facilitate this process.[7-12] The past few years have seen substantial study on the metal-based frameworks of Mannich bases, partly owing to the ligands' exceptional specificity for various transition metal ions. Such complexes exhibit a pronounced tendency to develop, resulting in molecules with substantial anti-cancer and anti-malarial effects. The simple synthetic procedure, versatility, and many uses have maintained Mannich base complexes as a significant and extensively researched field. Its influence on the advancement of coordination chemistry is well shown in the literature, underscoring the essential function of those metal-based complexes in the field's progression.[13-18] Comprehensive literature on the biological, chemical, and toxicological characteristics of Mannich bases, which have diverse uses as medicinal agents, dispersants in greases, and polymers. This is shown by a literature study on Mannich responses. Examining the structure and binding characteristics of various Mannich base complexes may significantly enhance the comprehension of intricate biotic functions.[19-21] Mosquitoes are essential insects due to their function as vectors in spreading illnesses.[22] They may transmit illnesses such as Japanese encephalitis, yellow fever, malaria, lumpy skin disease, filariasis, West Nile fever, and dengue.[23-27] In the past few decades, dengue viruses, transmitted through infectious female Culicidae mosquitoes, particularly *Aedes albopictus* and *Aedes aegypti*, have emerged as a significant worldwide healthcare concern.[28-30] Gibbons recognized *A. aegypti* as the principal transmitter of arboviral contagions caused by the dengue virus in developed countries.[31] Globally, annually, 50 to 100 million individuals get the illness, with about 2.5 % of these instances culminating in mortality.[32] Olfaction is crucial for organisms, facilitating food identification, host-seeking, reproduction, and predator recognition.[33] The transfer of odorants to olfactory receptors was expedited by odorant-binding proteins (OBPs), hence initiating signal transduction.[34,35] OBPs function as transporters of biochemical impulses to the olfactory receptors (ORs) for processing before neuronal transmission. *Culex quinquefasciatus*, *Anopheles gambiae*, and *Aedes aegypti* are prevalent transmitters of filariasis, encephalitis, and malaria as well.[36,37] Mosquito odorant-binding proteins (OBPs) exhibit a remarkable pH-dependent mechanism for binding and releasing odorants, capable of binding at a basic pH of 6.5 and transporting and releasing them at an acidic pH of 4.5.[38] The present research focused on *Culex quinquefasciatus* (CquiOBP1) (PDB code: 3OGN). This is distinctive due to its abbreviated C-boundary, contrasting with the domestic silk moths, Antheraea polyphemus (ApolPBP), and Bombyx mori (BmorPBP) that possess a C-boundary incorporated into the dominant cavity wall.[39] The CquiOBP1 complexes and oviposition pheromone exhibit weak binding at pH 5, nevertheless, high binding at pH 7.[40] An investigation of the mechanism of CquiOBP1 may be beneficial due to the strong correlation between experimental and theoretical findings. Consequently, we designated the OBP of *C. quinquefasciatus* as the desired target for docking investigations. Keep this in mind, we present the fabrication of a novel Mannich base and its complexes comprising Fe(II), Cu(II), Co(II), Ni(II), and Mn(II). Characterisation studies of all complexes were conducted using suitable methodologies. All metal complexes were evaluated for larvicidal efficacy towards *C. quinquefasciatus* larvae and for harmfulness towards marine fishes.

EXPERIMENTAL

Chemistry

The utilised substances were acquired from commercially available vendors and employed as supplied. The NMR spectra (^{1}H and ^{13}C) for the ligand were obtained in $CDCl_3$ using a Bruker 300 MHz instrument employing tetramethylsilane (TMS) as the benchmark. The IR spectra of the substances were obtained via KBr and CsI discs in the range of 4000–400 cm^{-1} on a Shimadzu FT-IR Spectrometer (FTIR-600). The electrospray (+) mass spectrophotometer was analysed using a Sciex ESI mass spectrometer. Melting points were ascertained with an electrothermal Stuart device, model SMP40. The UV-Vis spectra were obtained utilising a Shimadzu UV-160 throughout the wavelength range of 800-200 nm in DMSO solvents. Molar conductivity tests of the complexes were conducted at ambient temperature for 10^{-3} M solutions of the compounds in DMSO, utilising a digital conductivity meter Eutech Device Cyber Scan Con 510. Magnetic moments at 306 K were assessed using a magnetic susceptibility balance from Johnson Matthey.

Synthesis of Ligand (L1)

A solution was made in a round-bottom flask through combining a mixture of salicylaldehyde (2.4 mL, 0.02 mol), ethylenediamine (1.2 mL, 0.02 mol), and thiobarbituric acid (2.9 g, 0.02 mol) in ethanolic medium. At ambient temperature, the R.B. flask was positioned in a magnetic stirrer and stirred at 1000

rpm for roughly 30 minutes. The reaction's development was evaluated using thin-layer chromatography (TLC). Upon termination of the chemical reaction delineated via TLC, the resulting substance was submerged in crushed ice. The yellow crude substance was subjected to filtration and drying. The crude product was purified through recrystallisation using hot ethanol. Scheme-1 depicts the synthetic sequence of ligand (L1).

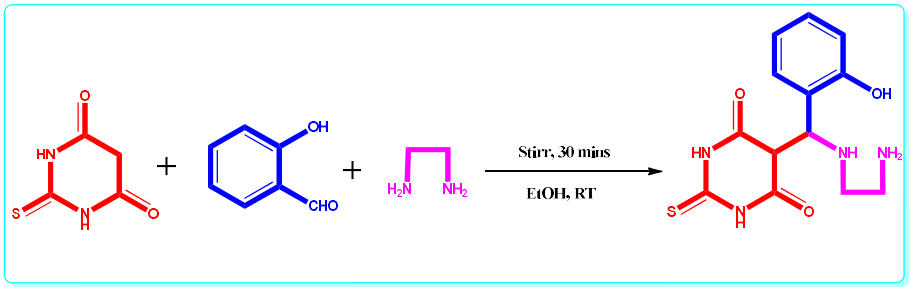

Scheme-1: Synthesis of Ligand (L1)

5-(((2-aminoethyl)amino)(2-hydroxyphenyl)methyl)-2-thioxodihydropyrimidine-4,6(1H,5H)-dione (L1)

Yellow solid; mw: 308.35; mp: 236°C; Elemental analysis: Anal. Calcd. for $C_{13}H_{16}N_4O_3S$: C, 50.64; H, 5.23; N, 18.17 %. Found: C, 50.62; H, 5.20; N, 18.20%; IR (KBr cm^{-1}) ν_{max}: 3435 (OH), 3163 (NH), 2950 (Ph_{str}), 1638 (C=O), 1240 (C=S); ^{1}H NMR (400 MHz, $CDCl_3$) δ 10.80 (s, 1H, OH), 9.80 (s, 1H, NH), 8.00 (s, 2H, NH), 7.12-6.90 (m, 4H, Ph-OH), 5.11 (s, 2H, NH_2), 4.62 (s, 1H, -CH-Ph), 3.99 (s, 1H, CH-CH-NH), 2.61 (t, 2H, J = 2.8 Hz, $-CH_2$), 1.42 (t, 2H, J = 2.8 Hz, $-CH_2$); ^{13}C NMR (100 MHz, $CDCl_3$) δ 181.0 (C=S, 1C), 172.0 (C=O, 2C), 153.0, 136.4, 128.2, 125.7, 121.1, 115.7 (Ph ring, 6C), 59.0 (CH-CH-Ph, 1C), 48.3 (CH-Ph, 1C), 37.8 ($-CH_2$-NH, 1C), 29.3 ($-CH_2$-NH_2, 1C); EI-MS: m/z 309.09 (M^+, 17%).

Synthesis of Metal Complexes (1-5)

Metal complexes of the $[M(L1)_2Cl_2]$ setting up, through M denoting Fe(II), Ni(II), Co(II), Mn(II), and Cu(II) were produced by introducing a solution of the metal precursor $MCl_2.H_2O$ (1 mmol, 1 eq) in 10 mL of ethanol to a solution of the same ligand **L1** (2.0 mmol) in 10 mL of ethanol. The solution was swirled and refluxed in an oil bath for 3 hrs. The resultant suspension, which yielded a solid precipitate, was subjected to filtration, wash away by ethanol, and dried under vacuum to isolate the complexes (**1-5**). The metal complexes have been purified through column chromatography utilising an eluent formulation of DCM:CH_3CN: CH_3OH (2:3:5 v/v) on silica gel. Metal complexes (**1-5**) were synthesised following the methodology outlined in Scheme-2.

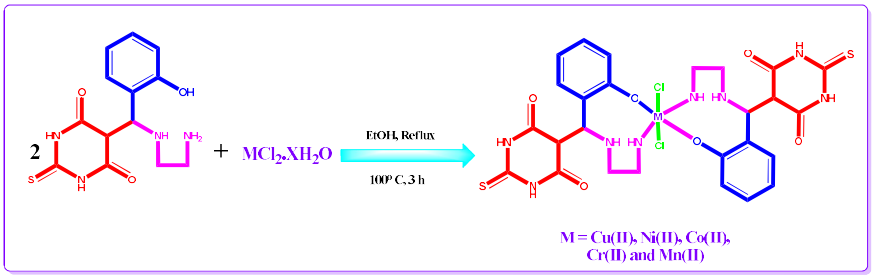

Scheme-2: Synthesis of Metal Complexes (1-5)

Solubility Measurements

The soluble nature of the complexes and ligand in protic and aprotic solvents has been determined. Studies utilised ethanol, water, chloroform, and dimethyl sulfoxide as solvents. Subsequent experiments were conducted based on the outcomes of the solubility evaluations.

Magnetic Susceptibility Measurement

The combination of magnetic susceptibility investigations and electronic spectra can be employed to determine the structure of the complex. Magnetic characteristics can be utilised to ascertain the stereochemistry of a metal ion complex with d^5, d^6, d^7, d^8, or d^9 electron configuration, specifically whether

it adopts a tetrahedral, square planar, or octahedral arrangement. Additionally, these parameters can indicate if the complex is spin-free or spin-paired. The magnetic properties of the metal atoms in the current complexes were examined using a Gouy magnetic balance to identify the most favourable magnetic moment for each atom at room temperature. The Gouy tube was standardized through mercury(II) tetrathiocyanatocobaltate(II), also known as $Hg[Co(SCN)_4]$. The diamagnetic modifications for various atomic and structural components were determined utilising Pascal's constants. The effective magnetic moment ($\mu_{eff.}$) was determined based on the molar magnetic susceptibilities (Mcorr) of the complexes using Curie's formula, $\mu_{eff} = 2.84\ [Mcorr\ T]^{1/2}$ B.M., where T represents the ambient temperature at which the measurements were made. The number of metal ions with unpaired electrons, 'n', can be calculated by analysing its effective magnetic moment, eff. The equation $\mu S = [n\ (n+2)]^{½}$ demonstrates the contribution of the electronic spin effect (S) to the moment.

Larvicidal Activity

Evaluations were conducted using a binary dead/alive criterion. Assessments are conducted on a percentage measure from 0 to 100, where 0 signifies no action and 100 represents complete death. The larvicidal efficacy of Mannich base ligand (**L1**) and its corresponding complexes (**1-5**) were assessed at concentrations of 100, 75, 50, and 25 µg/mL towards fourth-instar *Culex quinquefasciatus* using the water immersion technique, under settings of relative moisture of 40–60%, a photoperiod of 14:10 (dark: light), and at ambient temperature.[41] All test containers carrying 20 *Culex quinquefasciatus* larvae were assessed 24 hours post-treatment. The outcomes were documented as average percentage mortality. The bioassay was conducted thrice, and the bioactivity outcome was the mean of these duplicates. The commercial pesticide permethrin was evaluated as a control agent under identical conditions. The LC_{50} values of certain active title substances were assessed utilising the statistical program SPSS version 16.0.

Antifeedant Activity

The toxicity of Mannich base ligand (**L1**) and its complexes (**1-5**) was assessed through antifeedant screening using previously published literature with slight modifications.[42] Fishes (1.5–2.0 cm) of aquatic adapted *Oreochromis mossambicus* were utilized for assessing antifeedant activity. Ten fish were placed in testing and standard glassware containers, all bearing one litre of seawater and the required amount of the substance. Reflex alterations and mortality were noted immediately. Following a 24-hour exposure period, the quantities of deceased and surviving fish were enumerated.

Molecular Docking Methods

Ligand and Protein Preparation

The ligand (**L1**), complexes (**1-5**), and control permethrin were modelled with ChemDraw Ultra 12.0, and their energy was reduced utilising Chem3D Pro 12.0 software. The resulting structures have been retained in PDB format for docking evaluation. Both Mannich base and the complexes they form are collectively mentioned as ligands in the context of docking methodology. This study investigated the protein databank to obtain the crystal structures of proteins associated with certain experimental biological experiments. The structure of mosquito OBP (PDB ID: 3OGN) was utilised for the larvicidal assay. Within the crystal structure, a single protein chain was chosen and preserved as the target protein for docking, whereas water molecules, heteroatoms, distinct ligands, and additional chains were removed. Meanwhile, the co-crystallized ligand in the target protein was partitioned for a reserve of less than 5 Å. The amino acid sequence inside this zone was recorded and considered as the range of the binding cavity for an inhibitory effect.

Docking Procedure

The docking studies were performed utilising the Autodock Vina simulated screening program.[43] Initially, the protein construct (receptor) was put onto Vina and subsequently transformed into a macromolecule by transforming it into a PDB and pdbqt set-up for the purpose of docking. The grid box of the target receptor was defined at center_x: 18.681, center_y: 49.66, and center_z: 11.409 through dimensions size_x: 22, size_y: 20, and size_z: 22. The grid has a uniform spacing of 1.0 Å between each point. An integer value of 8 has been allocated to the exhaustiveness score. The remaining parameters were configured according to their default settings for Vina docking and were not explicitly defined. The ligand with the lowest docking

score is regarded as the compound with the greatest activity. Visual assessment of the docking results was conducted using the Discovery Studio Visualizer.

RESULTS AND DISCUSSION

Physical Data and Solubility

The solubility and physicochemical properties of the ligand (**L1**) and associated complexes (**1-5**) are detailed in Table-1. The solubility studies indicate that the tested substances exhibit superior solubility in aprotic solvents relative to protic solvents.

Table-1: Physical Data and Solubility of the Metal Complexes (1-5) and Ligand (L1)

Compound	Colour	Melting point (°C)	Solubility			
			Water	Ethanol	Chloroform	DMSO
Ligand (L1)	Yellow	228	Insoluble	Soluble	Sparingly soluble	Soluble
Copper complex (1)	Blue	180	Insoluble	Soluble	Insoluble	Soluble
Nickel complex (2)	Green	134	Insoluble	Soluble	Insoluble	Soluble
Cobalt complex (3)	Red	208	Insoluble	Soluble	Insoluble	Soluble
Iron complex (4)	Dark brown	176	Insoluble	Soluble	Insoluble	Soluble
Manganese complex(5)	Purple	153	Insoluble	Soluble	Insoluble	Soluble

Conductivity and Magnetic Susceptibility Measurements

The neutral (non-electrolytic) characteristics of the complexes were confirmed by assessing the conductivity nature of their respective 10^{-3} M solutions in DMSO. The metal complexes (**1-5**) exhibited a molar conductance between 14 - 26 $\Omega^{-1}mol^{-1}cm^2$. The conductivity experiment results demonstrated that chloride ions demonstrate complexation tendency with metal ions, suggesting they act as ligands rather than as separate ions. The arrangement of the produced complexes may be influenced through the ligand-metal proportions (2:1) and the kinds of electrolytes employed in the conductivity evaluation. The magnetic moment of Fe(II), Ni(II), Mn(II), and Co(II) complexes demonstrates an octahedral geometry and high-spin. The diminished magnetic moment of the Cu(II) complex indicates a low-spin, deformed octahedral geometry. Table-2 displays the electrical conductivity and magnetic properties of metallic complexes (**1-5**).

Table-2: Conductance and Magnetic Properties of Metal Complexes (1-5) with Ligand (L1)

S. No	Compounds	Conductance ($\Omega^{-1}mol^{-1}cm^2$)	Magnetic Susceptibility (μ_{eff}. B.M)
1.	Copper complex (1)	14	2.20
2.	Nickel complex (2)	25	3.54
3.	Cobalt complex (3)	23	5.68
4.	Iron complex (4)	26	4.32
5.	Manganese complex (5)	22	5.28

NMR Spectral Studies of Ligand (L1)

The signal at 9.80 ppm resembles the -NH hydrogens of the thiobarbituric acid moiety. The phenyl ring protons display a multiplet at 7.12-6.90 ppm. The $-CH_2$ protons connected to the amine hydrogen atoms of ethylenediamine and the salicylaldehyde are detected as a signal at 4.62 ppm, whilst the hydroxyl proton resonates at 10.80 ppm. The nonappearance of a signal for the proton of the secondary amine $–NH_2$, which was detached during the Mannich reaction, helps substantiate synthesis of the ligand. The carbon atoms of the phenyl ring had signals at 153.0-115.7 ppm.

The existence of a signal at 48.3 ppm signifies that the $-CH_2$ is bonded to the amine hydrogens of ethylenediamine and salicylaldehyde. The peaks at 181.0 and 172.0 ppm belong to the thiocarbonyl and carbonyl carbons of the thiobarbituric acid group, respectively. The carbons from the ethylenediamine moiety were confirmed by the peaks seen at 37.8 and 29.3 ppm. The ^1H and ^{13}C NMR spectra of the Mannich base ligand (**L1**) are accessible in Fig.-1 and Fig.-2.

Mass Spectral Studies of Ligand (L1)

The mass spectra of the Mannich base ligand (**L1**) are illustrated in Fig.-3. The mass spectra of ligand (**L1**) displayed discrete peaks at molecular weights that complied closely with theoretically expected values. The molecular weight of ligand (**L1**) was experimentally determined to be 308.35, a result corroborated by mass spectral analysis indicating the m/z value of 309.23. The molecular ion signal remained observed at a m/z value of 309.23.

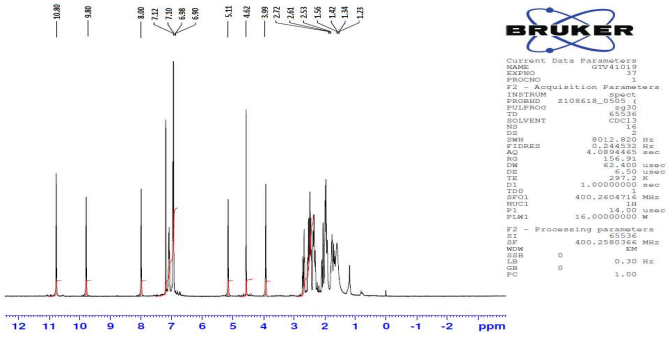

Fig.-1: ^{1}H-NMR Spectra of Ligand (L1)

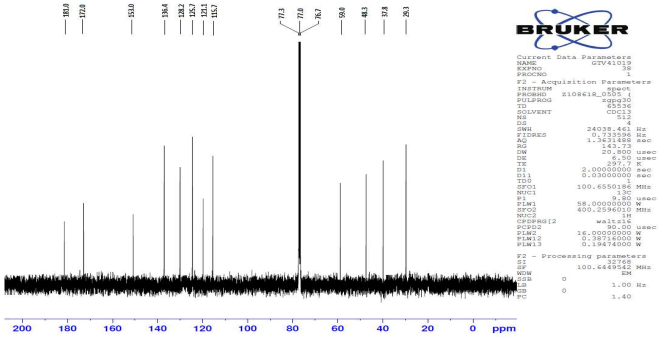

Fig.-2: ^{13}C-NMR pectra of Ligand (L1)

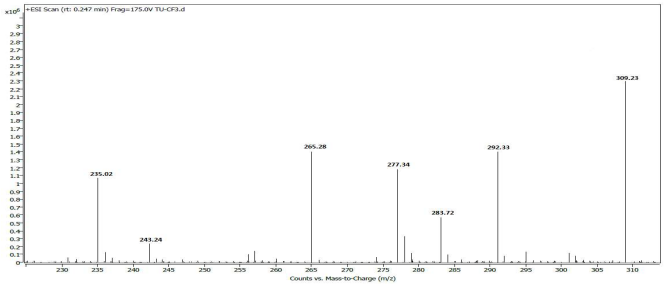

Fig.-3: Mass Spectra of Ligand (L1)

IR Spectra

A notable finding in the ligand FT-IR spectra (Fig.-4) is the occurrence of prominent peaks at 3435 and 3163 cm^{-1}, corresponding to the νOH and NH amine groups, respectively. A shift to higher frequency was noted in the N-H and O-H bands of all complexes (Fig.-5 to 9), signifying the participation of hydroxyl oxygen and amine nitrogen in interactions with the metal ions. The FT-IR ligand (**L1**) exhibits peaks at 1638 and 1240 cm^{-1}, specifying the existence of carbonyl and thiocarbonyl groups. The nonappearance of significant changes in the carbonyl and thiocarbonyl peaks in the FT-IR spectra of metal complexes (**1-5**) suggests that the carbonyl and thiocarbonyl groups do not engage in coordination with metal ions. The manifestation of bands in the wavenumber array of 783-753 cm^{-1} signifies the presence of the M-N connection. The existence of distinct peaks at a wavenumber of 640-598 cm^{-1}, associated with the M-O bond, signifies the formation of metal complexes (**1-5**). The M-Cl bond is indicated by a distinct peak around the spectral range of 488-468 cm^{-1}. Table-3 presents the FT-IR spectral results for complexes 1-5 and ligand L1.

Table-3: FT-IR Spectral Data

Compound		IR stretching frequency (cm^{-1})					
	-OH	-NH	-C=O	-C=S	M-N	M-O	M-Cl
Ligand (L1)	3435	3163	1638	1240	-	-	-
Copper complex (1)	3470	3276	1639	1238	783	639	476
Nickel complex (2)	3478	3214	1640	1241	753	640	468
Cobalt complex (3)	3461	3264	1641	1240	757	635	474
Iron complex (4)	3453	3184	1638	1239	754	620	488
Manganese complex (5)	3240	3276	1641	1240	761	598	484

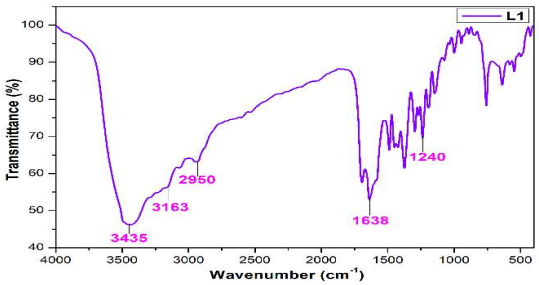

Fig.-4: FT-IR Spectra of Ligand L1

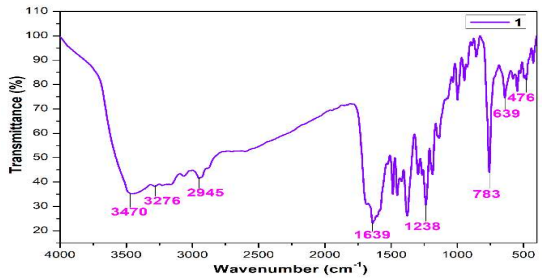

Fig.-5: FT-IR Spectra of Copper Complex 1

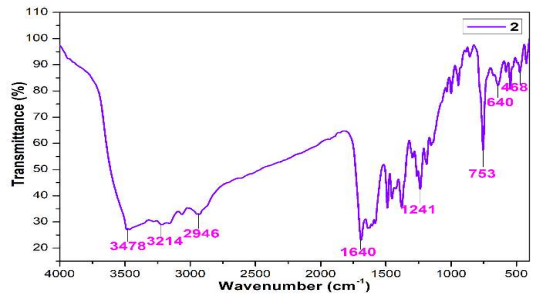

Fig.-6: FT-IR Spectra of Nickel Complex 2

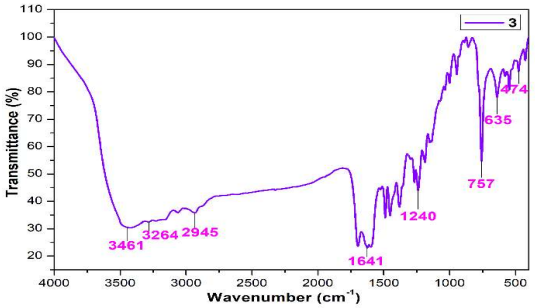

Fig.-7: FT-IR Spectra of Cobalt Complex 3

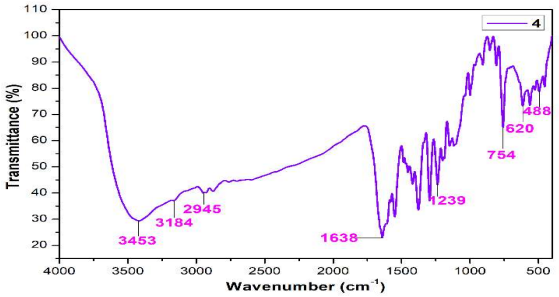

Fig.-8: FT-IR Spectra of Iron Complex 4

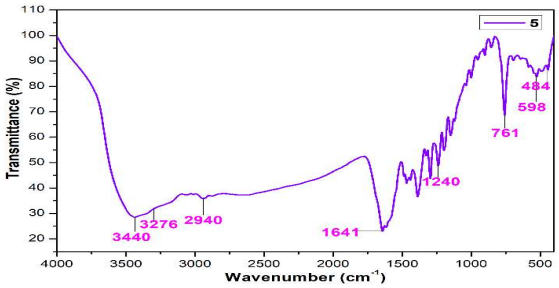

Fig.-9: FT-IR Spectra of Manganese Complex 5

UV-Visible Spectra

The electronic spectrum of ligand (**L1**) displayed two absorbance maxima at 225 nm and 296 nm, conforming to π→π* and n→π* shifts, individually (Fig.-10). The spectra of the complexes in DMSO displayed three different peaks. Intra-ligand changes were discerned by two separate bands detected at wavelengths of 268-298 nm and 330-376 nm. The compound was validated by the band found in the 406-438 nm range, attributable to LMCT transitions (Fig.-11 to 15).

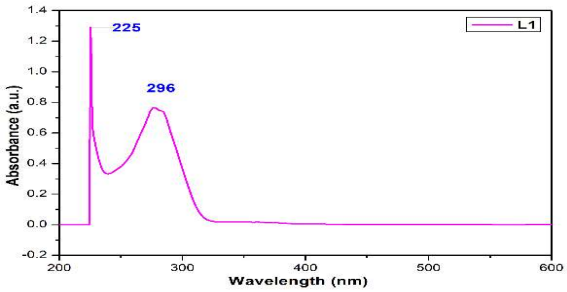

Fig.-10: UV-Visible Spectrum of Ligand L1

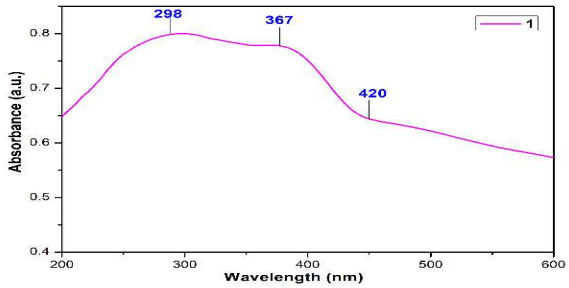

Fig.-11: UV-Visible Spectrum of Complex 1

EPR Spectra

Studies on EPR spectra can elucidate the formation of ligand-metal relations and the assembly of unpaired and paired electrons. Copper (II) complexes demonstrate unique properties in coordination chemistry, showcasing several geometries, for instance, square pyramidal, square planar, tetrahedral, and octahedral, which can be evident through EPR spectra. The EPR characteristics G, g_{avg}, $g^{\perp}$, and $g_{\parallel}$ are utilised to

ascertain whether a complex possesses an octahedral or tetrahedral configuration. The occurrence of an unpaired electron in the d_x^2-$_y^2$ orbital is validated by the condition that the $g_{\parallel}$ exceeds the $g^{\perp}$, that is, greater than 2.0023.

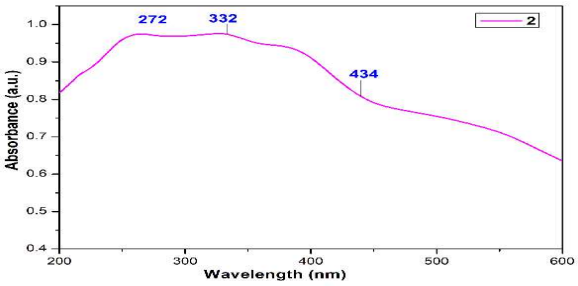

Fig.-12: UV-Visible Spectrum of Complex 2

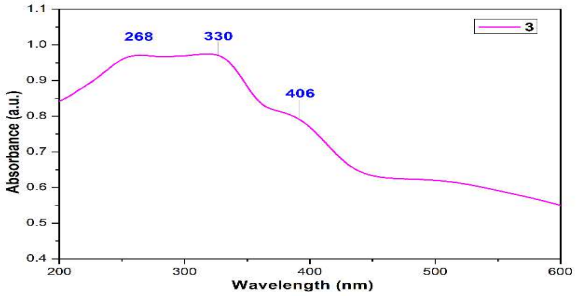

Fig.-13: UV-Visible Spectrum of Complex 3

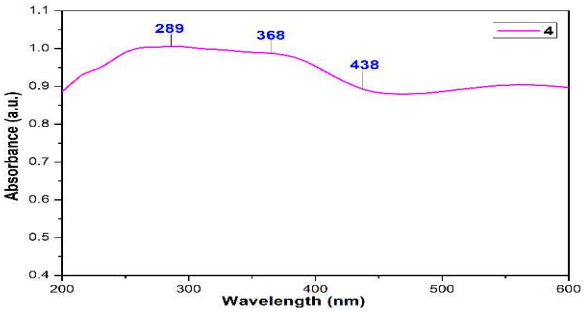

Fig.-14: UV-Visible Spectrum of Complex 4

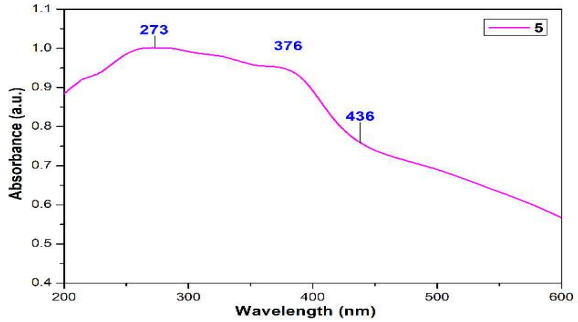

Fig.-15: UV-Visible Spectrum of Complex 5

The $g_{\parallel}$ and $g^{\perp}$ values for the copper complex are recorded as 2.2561 and 2.0742, respectively. The covalent character is signified by a $g_{\parallel}$ value below 2.3, whereas an ionic character is indicated by a $g_{\parallel}$ value over 2.3. The $g_{\parallel}$ value (2.2561) is clearly below 2.3, signifying that the copper complex exhibits a covalent nature. Hathaway asserts that G values below four imply substantial interaction among metal centres, whilst G values beyond four denote minimal charge transfer. In this instance, the G value is 3.45, signifying that the charge transfer is considerable. The Cu (II) complex has a distorted octahedral geometry, as evidenced by its EPR spectra. Fig.-16 shows the EPR spectra of copper complex (**1**).

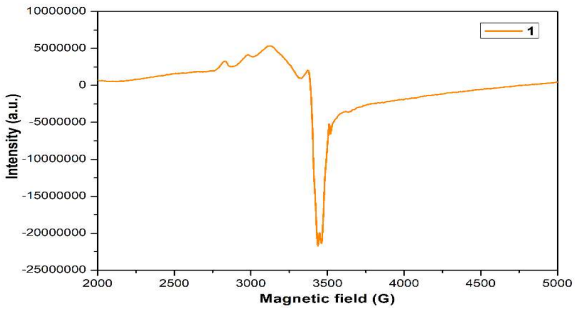

Fig.-16: EPR Spectra of Copper Complex 1

Larvicidal Activity

The ligand (**L1**) and corresponding complexes (**1-5**) were assessed for larvicidal efficacy towards 4th instar *C. quinquefasciatus* larvae. The Mannich base ligand (**L1**) exhibited moderate larvicidal action, with an LC_{50} value of 39.55 µg/mL, related to the standard permethrin (LC_{50} = 26.13 µg/mL). The synthesised metal complexes (**1-5**) exhibited superior larvicidal action than the free ligand (**L1**). The larvicidal efficacy of the free ligand was improved through complexation with metal ions. Among the synthesised complexes (**1-5**), the manganese complex (**5**) exhibited superior larvicidal activity (LC_{50} = 16.25 µg/mL) compared to the free ligand (LC_{50} = 39.55 µg/mL) and the control permethrin (LC_{50} = 26.13 µg/mL). The copper complex (**1**) and cobalt complex (**3**) exhibited notable larvicidal activity, having LC_{50} of 16.36 and 20.14 µg/mL, respectively, related to the standard permethrin (LC_{50} = 26.13 µg/mL). The nickel complex (**2**) and iron complex (**4**) exhibited moderate larvicidal activity, having LC_{50} of 32.85 and 35.60 µg/mL, respectively, compared to the control permethrin (LC_{50} = 26.13 µg/mL). The results are presented in Table-4.

Table-4: Larvicidal Activity

Compounds	Concentration (µg/mL) / Mortality (%)				LC_{50} (µg/mL)
	100	75	50	25	
Ligand (L1)	86±0.12	74±0.46	64±0.48	38±1.14	39.55
Copper complex (1)	72±1.20	64±1.23	56±1.30	42±0.46	16.36
Nickel complex (2)	100±0.00	86±0.96	70±0.28	34±1.89	32.85
Cobalt complex (3)	100±0.00	84±1.43	68±1.56	40±0.58	20.14
Iron complex (4)	78±1.61	62±0.62	54±0.34	28±1.26	35.60
Manganese complex (5)	80±1.14	70±1.30	62±1.46	46±0.33	16.25
Permethrin	84±0.87	70±0.27	52±0.58	40±1.24	26.13

[a]Values are the means of three replicates ± SD.

Antifeedant Activity (Ichthyotoxicity Activity)

The toxic effects of the ligand (**L1**) and corresponding metallic complexes (**1-5**) were measured using the marine fish, *Oreochromis mossambicus*. The synthesised Mannich base ligand exhibited more toxicity than its metal complexes. The harmful effects of the unbound ligand decreased during complexation with metal ions. The notable larvicidal complexes (**1**, **3**, **5**) exhibited lower toxicities in non-target aquatic species (*Oreochromis mossambicus*), with an LC_{50} value over 100 µg/mL. The moderate larvicidal complexes (**2** and **4**) showed greater toxicity (LC_{50} = 59.46 and 56.12 µg/mL) to non-target aquatic species and exhibited lower toxicity than the free ligand (LC_{50} = 51.40). The outcomes are displayed in Table-5.

Table-5: Antifeedant Action

Compounds	Concentration (µg/mL) / Mortality (%)				LC_{50} (µg/mL)
	100	75	50	25	
Ligand (L1)	90±0.21	70±1.35	54±0.12	24±1.76	51.40
Copper complex (1)	40±0.42	28±1.25	16±0.34	10±1.63	>100
Nickel complex (2)	80±1.23	68±0.42	42±1.38	20±0.74	59.46
Cobalt complex (3)	43±0.45	32±0.46	24±1.38	12±0.42	>100
Iron complex (4)	84±1.28	68±0.26	40±1.34	28±0.74	56.12
Manganese complex (5)	46±1.24	30±1.52	14±0.76	8±1.23	>100

[a]Values are the means of three replicates ± SD

***In-silico* Docking**

The docking interactions of the Mannich base ligand (**L1**), metal complexes (**1-5**), and the standard permethrin were examined utilising the 3OGN protein and AutoDock Vina modelling program. The Mannich base ligand (**L1**) exhibited lower larvicidal efficacy, having a docking score of -5.8 kcal/mol, related to its corresponding complexes (**1-5**) and the standard permethrin (Binding score = -7.6 kcal/mol). The Mannich base ligand (**L1**) didn't generate any hydrogen bond connections with the protein. The residues of amino acids Leu124, Trp114, Met91, and Leu76 participated in hydrophobic contacts. The manganese complex (**5**) exhibited superior larvicidal efficacy (Binding score = -9.8 kcal/mol), surpassing that of the other complexes (**1-4**) and the standard permethrin (Binding score = -7.6 kcal/mol). The manganese complex (**5**) failed to establish a hydrogen bond contact with the protein. The amino acids Ser79 and Ala62 participated in hydrophobic interactions. The standard permethrin exhibited substantial larvicidal efficacy (Binding score = -7.6 kcal/mol), surpassing that of the Mannich base ligand (**L1**) at -5.8 kcal/mol, the nickel complex (**2**) at -6.2 kcal/mol, and the iron complex (**4**) at -6.7 kcal/mol. The standard permethrin, too, failed to establish any hydrogen bond interactions with the 3OGN receptor, but the amino acids Leu124, Leu19, Phe123, Leu73, Leu80, Leu76, Met89, His77, His111, Ala88, Gly92, Trp114, Phe59, and Leu15 participated in hydrophobic contacts. Figs. 17-23 illustrate the interactions among the Mannich base ligand (**L1**), metal complexes (**1-5**), and the control permethrin with the 3OGN receptor. The findings indicate that manganese complex (**5**) restricted the function of the OBP of *C. quinquefasciatus* with greater efficiency than the other complexes, free ligand, and control permethrin. Table-6 highlights the findings.

Table-6: Molecular Docking Interaction of Ligand (L1), Metal Complexes (1-5), and Control Permethrin Towards OBP Of 3OGN

Compounds	Mosquito OBP of 3OGN		
	Binding score (kcal/mol)	No. of H-bonds	H-bonding residues
Mannich base ligand (L1)	-5.8	-	-
Copper complex (1)	-8.9	2	Lys63, Ser79
Nickel complex (2)	-6.2	2	Ala62, Asp78
Cobalt complex (3)	-7.4	2	Val125
Iron complex (4)	-6.7	-	-
Manganese complex (5)	-9.8	-	-
Permethrin	-7.6	-	-

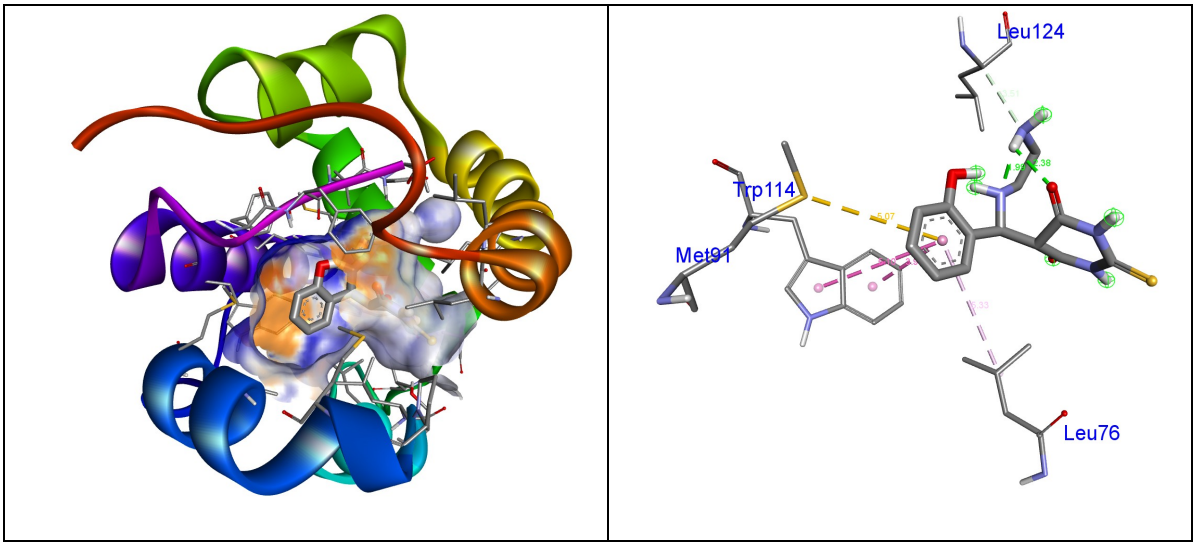

Fig.-17: Interaction Modes of Mannich Base Ligand (L1) into the Binding Pocket of 3OGN

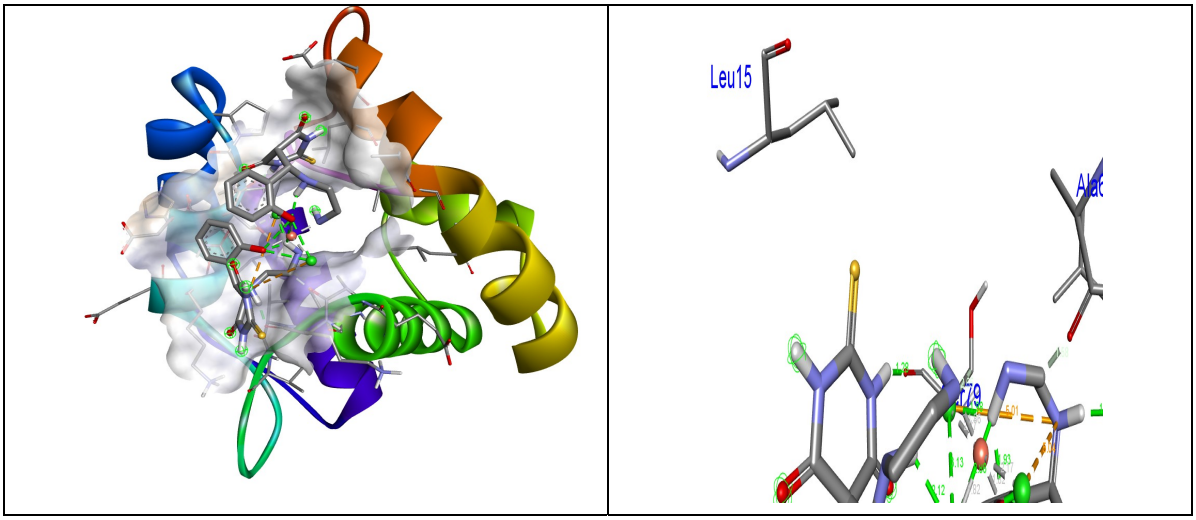

Fig.-18: Interactions of Copper Complex (1) into the Binding Pocket of 3OGN

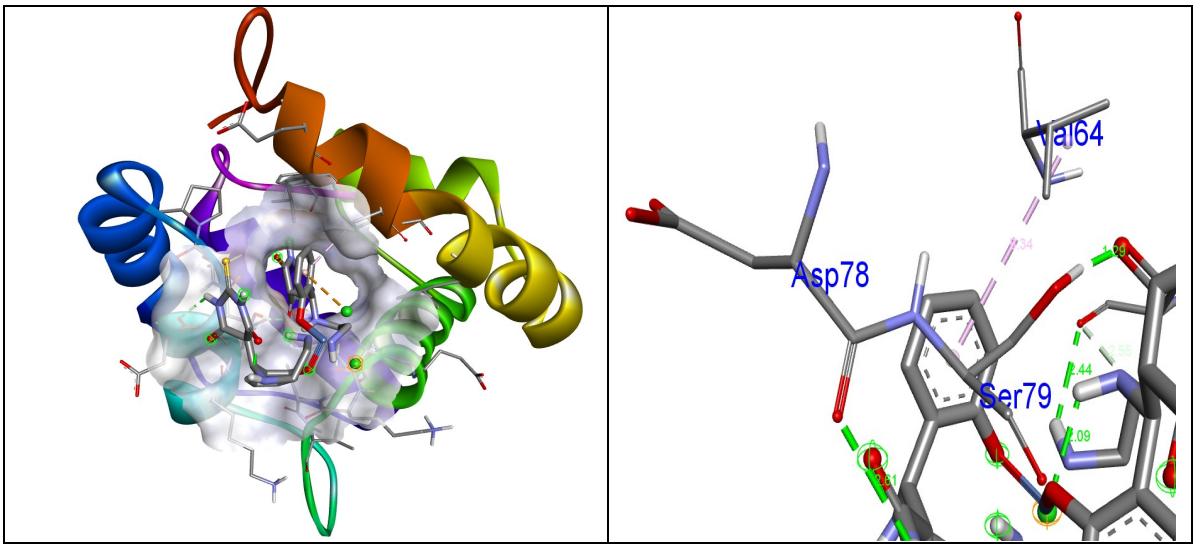

Fig.-19: Interactions of Nickel Complex (2) into the Binding Pocket of 3OGN

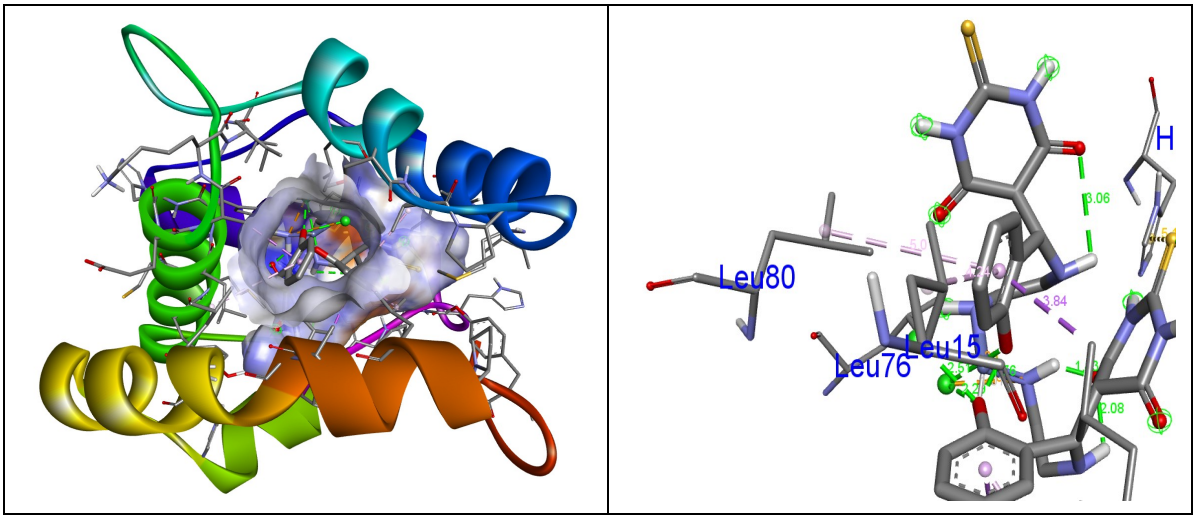

Fig.-20: Interactions of Cobalt Complex (3) into the Binding Pocket of 3OGN

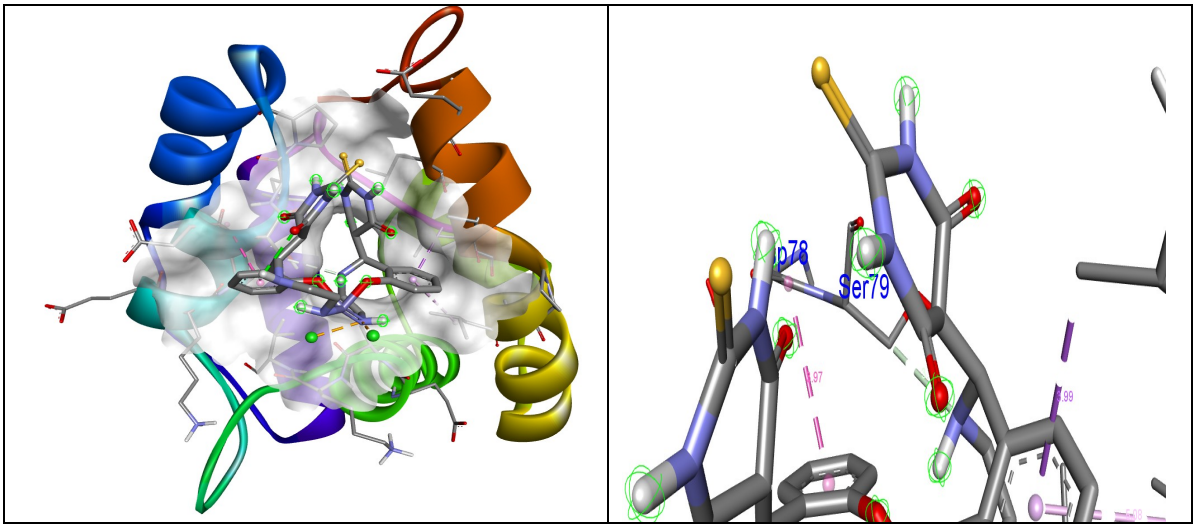

Fig.-21: Interactions of Iron Complex (4) into the Binding Pocket of 3OGN

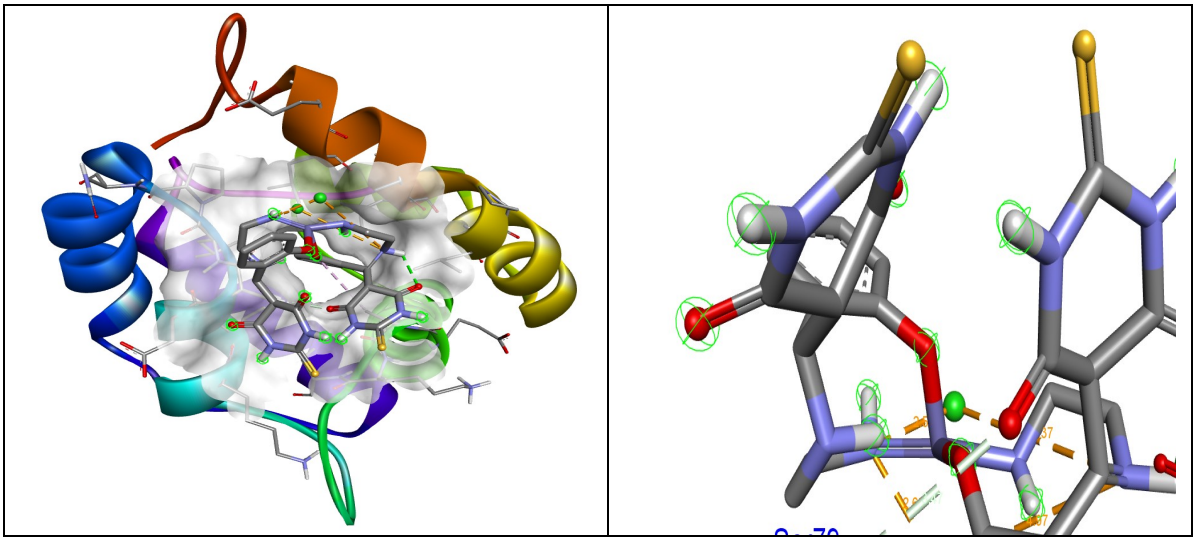

Fig.-22: Interactions of Manganese Complex (5) into the Binding Pocket of 3OGN

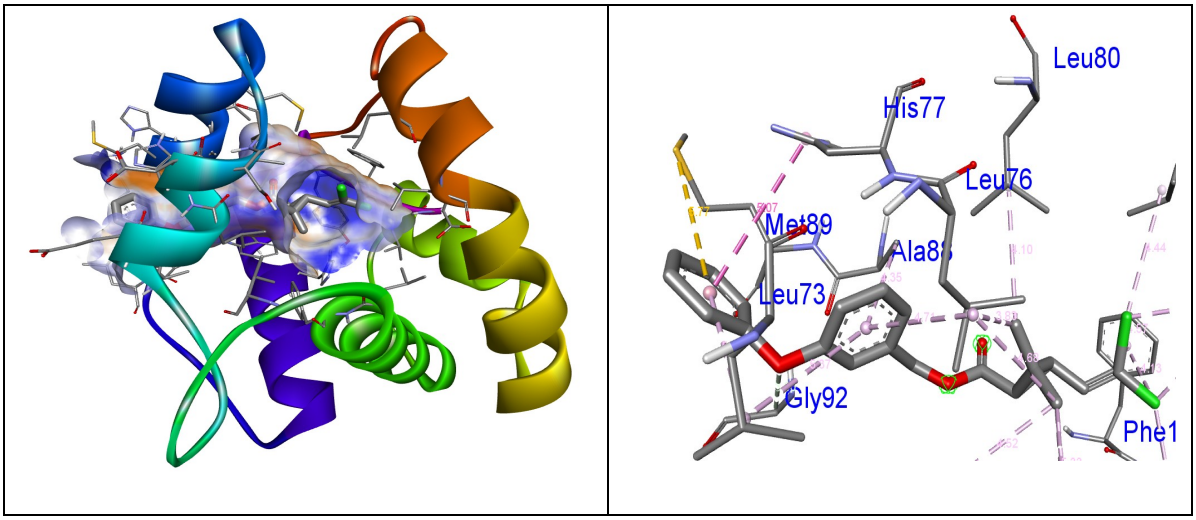

Fig.-23: Interactions of Standard Permethrin into the Binding Pocket of 3OGN

CONCLUSION

This paper delineates the coordination characteristic of a Mannich base ligand synthesised via the interaction of thiobarbituric acid, salicylaldehyde, and ethylenediamine. Complexes of Fe (II), Cu (II), Co (II), Mn (II) and Ni (II) were synthesised utilising the aforementioned ligand and characterised through magnetic, spectroscopic, and analytical facts. The ligand coordinates to the metal atom through the oxygen of salicylaldehyde and the nitrogen of ethylenediamine, functioning as a neutral bidentate ligand. The octahedral geometry was displayed by all the synthesized complexes. The ligand and its metal complexes have notable larvicidal action against mosquitoes. The Mn (II) complex exhibited effective larvicidal action while demonstrating reduced toxicity to non-target aquatic organisms, specifically marine fish. The mechanism of action of the complexes and the forecast of its effective binding to the receptor were determined using molecular docking techniques. The obtained results aligned with findings from experiments.

ACKNOWLEDGMENTS

The Authors acknowledge their respective managements for providing the opportunity to accomplish this research.

CONFLICT OF INTERESTS

The authors assert that no conflict of interest exists.

AUTHOR CONTRIBUTIONS

All the authors contributed significantly to this manuscript, participated in reviewing/editing and approved the final draft for publication. The research profile of the authors can be verified from their ORCID ids, given below:

Devaraj Kavitha https://orcid.org/0009-0001-6080-4233
Velayutham Gurunathan https://orcid.org/0009-0009-2547-5276
Karumalaiyan Palanisamy https://orcid.org/0000-0002-4745-8583
Sangilimuthu Aruna Devi https://orcid.org/0000-0001-6914-1985

REFERENCES

1. H. A. Bhatti, R. Rubina, F. Rashid, S. Zaib, J. Iqbal, and A. Hameed, *Natural Resources for Human Health*, **2(2),** 100(2022), https://doi.org/10.53365/nrfhh/141866
2. H. Sharghi, S. F. Razavi, M. Aberi, F. Tavakoli, and M. Shekouhy, *ChemistrySelect*, **5(9)**, 2662(2020), https://doi.org/10.1002/slct.201904700
3. M. Strzelecka, T. Glomb, M. Drąg-Zalesińska, J. Kulbacka, A. Szewczyk, J. Saczko, and P. Świątek, *International Journal of Molecular Sciences*, **23(19)**, 11173(2022), https://doi.org/10.3390/ijms231911173
4. A. M. Al-Khazraji, and R. A. Al Hassani, *Reviews in Pharmacy*, **11(5)**, 535(2020), https://doi.org/10.31838/srp.2020.5.71
5. S. Janowska, S. Andrzejczuk, P. Gawryś, and M. Wujec, *Molecules*, **28(14)**, 5562(2023), https://doi.org/10.3390/molecules28145562
6. H. J. Abaas, and M. J. Al-Jeboori, In *Journal of Physics: Conference Series,* **1879(22074)**, 3(2021), http://dx.doi.org/10.21931/RB/2023.08.02.15
7. E. M. Afsah, S. S. Elmorsy, S. M. Abdelmageed, and Z. E. Zaki, *Zeitschrift für Naturforschung B*, **70(6)**, 393(2015), https://doi.org/10.1515/znb-2014-0262
8. B. Biersack, K. Ahmed, S. Padhye, and R. Schobert, *Expert Opinion on Drug Discovery*, **13(1)**, 39(2018), https://doi.org/10.1080/17460441.2018.1403420
9. E. J. Waheed, A. Al-Khazraji, and A. A. Ahmed, *Journal of Applied Sciences and Nanotechnology*, **3(4)**, 42(2023), https://doi.org/10.53293/jasn.2023.7033.1228

10. A. M. Al-Khazraji, R. A. Al Hassani, and A. Ahmed, *Systematic Reviews in Pharmacy*, **11(5),** 525(2020), http://dx.doi.org/10.5530/srp.2019.2.04
11. A. M. Etheb and M. J. Al-Jeboori, *HIV Nursing,* **22(2),** 3659(2022).
12. H. A. Saleh, A. S. A. Abdul Rahman, and M. J. Al-Jeboori, *Biochemical and Cellular Archives*, **21(1)**, 159(2021).
13. G. B. Karthi, M. Y. Suvaikin, and C. Kalaivanan, *European Chemical Bulletin*, **12(1)**, 1391(2023).
14. S. M. Shakir, and Al-Majedy, *Journal of Applied Sciences and Nanotechnology*, **2(1)**, (2022), http://dx.doi.org/10.53293/jasn.2021.4164.1076
15. S. S. Raoof, and A. S. Sadiq, *Iraqi Journal of Science*, **63(12)**, 5086(2022), https://doi.org/10.24996/ijs.2022.63.12.1
16. A. Olyaei, M. Sadeghpour, and M. Khalaj, *RSC Advances*, **10(51)**, 30265(2020), https://doi.org/10.1039/D0RA05717G
17. R. Ranjan, B. K. Kundu, R. Kyarikwal, R. Ganguly, and S. Mukhopadhyay, *Applied Organometallic Chemistry*, **36(1)**, 6450(2022), https://doi.org/10.1002/aoc.6450
18. D. M. Nagrik, and U. S. Shelke, *Journal of Physics: Conference Series*, **1644(1)**, 012018(2020), https://doi.org/10.1088/1742-6596/1644/1/012018
19. A. M. A. Al-Khazraji, *Indonesian Journal of Chemistry*, **23(3)**, 754(2023), https://doi.org/10.22146/ijc.81272
20. A. A. Ahmed, E. J. Waheed, and A. T. Numan, *Journal of Physics: Conference Series,* **1660(1)**, 012109(2020), https://doi.org/10.1088/1742-6596/1660/1/012109
21. B. S. Al-Dobony, and A. Y. Al-Assafe, *Journal of Physics: Conference Series,* **1294(5)**, 052068(2019), https://doi.org/10.1088/1742-6596/1294/5/052068
22. M. Coetzee, *Transactions of the Royal Society of Tropical Medicine and Hygiene*, **108(4),** 179(2014), https://doi.org/10.1093/trstmh/tru020
23. A. Selim, A. Megahed, S. Kandeel, A. Alouffi, and M. M. Almutairi, *Scientific Reports*, **11(1)**, 20932(2021), https://doi.org/10.1038/s41598-021-00449-6
24. A. Selim, and A. Abdelhady, *Tropical Animal Health and Production*, **52(6),** 3147(2020), https://doi.org/10.1007/s11250-020-02339-x
25. A. Selim, E. Manaa, and H. Khater, *Comparative Immunology, Microbiology and Infectious Diseases*, **79**, 101699(2021), https://doi.org/10.1016/j.cimid.2021.101699
26. A. Selim, E. Manaa, and H. Khater, *Tropical Animal Health and Production*, **53(3)**, 350(2021), https://doi.org/10.1007/s11250-021-02786-0
27. A. Selim, H. A. Alafari, K. Attia, M. D. AlKahtani, F. M. Albohairy, and I. Elsohaby, *Scientific Reports*, **12(1)**, 8933(2022), https://doi.org/10.1038/s41598-022-12817-x
28. D. Hamady, N. B. Ruslan, A. H. Ahmad, C. S. M. Rawi, H. Ahmad, T. Satho, and S. AbuBakar, *Parasites and Vectors*, **6**, 1(2013), https://doi.org/10.1186/1756-3305-6-206
29. M. J. Conway, T. M. Colpitts, and E. Fikrig, *Annual Review of Virology*, **1(1)**, 71(2014), https://doi.org/10.1146/annurev-virology-031413-085513
30. M. M. Baz, A. Selim, I. T. Radwan, A. M. Alkhaibari, and H. F. Khater, *Scientific Reports*, **12(1)**, 4406(2022), https://doi.org/10.1038/s41598-022-08223-y
31. A. Selim, H. Almohammed, A. Abdelhady, A. Alouffi, and F. A. Alshammari, *Parasites and Vectors*, **14(1)**, 429(2021), https://doi.org/10.1186/s13071-021-04943-8
32. WHO. Dengue and severe dengue. Geneva: World Health Organisation (2014), http://www.who.int/media centre/ facts heets/ fs117/en/ , Accessed 14th April 2025.
33. A. Bazaes, J. Olivares and O. Schmachtenberg, *Journal of Chemical Ecology,* **39**, 451(2013), https://doi.org/10.1007/s10886-013-0268-1
34. C. A. De March and J. A. Golebiowski, *Biochimie*, **107**, 3(2014), https://doi.org/10.1016/j.biochi.2014.06.006
35. M. Pechlaner and C. Oostenbrink, *Journal of Chemical Information and Modeling,* **55**, 2633(2015), https://doi.org/10.1021/acs.jcim.5b00673
36. F. Chandre, F. Darriet, M. Darder, A. Cuany, J. Doannio, N. Pasteur and P. Guillet, *Medical and Veterinary Entomology,* **12(4)**, 359(1998), https://doi.org/10.1046/j.1365-2915.1998.00120.x

37. R. M. R. Barbosa, A. Furtado, L. Regis and W. S. Leal, *Brazil. Journal of Vector Ecology,* **35(1)**, 204(2010), https://doi.org/10.1111/j.1948-7134.2010.00078.x
38. E. Di Luccio, Y. Ishida, W. S. Leal and D. K. Wilson, *Plos One*, **8**, e53840(2013), https://doi.org/10.1371/journal.pone.0053840
39. Y. Mao, X. Xu, W. Xu, Y. Ishida, W. S. Leal, J. B. Ames, *Proceedings of the National Academy of Sciences,* **107**, 19102(2010), https://doi.org/10.1073/pnas.1012274107
40. W. S. Leal, R. Barbosa, W. Xu, Y. Ishida, Z. Syed, N. Latte, A. M. Chen, T. I. Morgan, A. J. Cornel and A. Furtado, *PLoS One*., **3(8)**, 3045(2008), https://doi.org/10.1371/journal.pone.0003045
41. X. Li, X. Yang, Z. Cui, Y. Li, H. He and Y. Ling, *Chinese Journal of Chemistry,* **28**, 1233(2010), https://doi.org/10.1002/cjoc.201090214
42. A. A. Mostafa, C. SathishKumar, A. A. Al-Askar, S. R. Sayed, R. Surendra Kumar, A. Idhayadhulla, *RSC Advances*, **9(44)**, 25533(2019), https://doi.org/10.1039/C9RA04496E
43. O. Trott and A. J. Olson, *Journal of Computational Chemistry,* **31**, 455(2010), https://doi.org/10.1002/jcc.21334

[RJC-9139/2024]